Measurements of Capacitor Noise

May 10th, 2013

Anna Czerepak

Physics 406

Spring 2013

1 Introduction

A capacitor is a familiar passive circuit component. Broadly defined, a capacitor is any two electrical conductors separated by an insulator (or a dielectric). The familiar ceramic disc capacitors are one example but capacitors manufactured today can be made out of any number of materials, geometries, dielectrics, or function via a variety of charge-storing mechanisms (the three most common being: polarization of a dielectric, a chemical redox reaction, and the usual electrostatic). Capacitors are common in most circuits, but little scientific research has been done on the question of what makes a capacitor 'musical'. In other words, what measurable properties (aside from listening to the sound produced by equipment with the capacitor installed) make one type, brand, or model of capacitor sound better or worse than another. In the simplest approximation, capacitors behave roughly ideally and capacitors with the same value for capacitance should be functionally identical. However, physical realities such as manufacturing defects, finite time responses, and non-linear behavior of the dielectric lead to a variety of capacitor behaviors that can vary widely from one type of capacitor to another.

Among musicians (and the musically-inclined), there are many opinions and casual guesses to what makes certain capacitors musical but to the author's knowledge, a rigorous scientific investigation of the topic has not been done (except for the work of Dr. S. Errede in PHYS406). The goal of this project was to build a circuit with which to test these capacitors and try to extract quantities from the measured data that correlate with 'musicality'. The requirements for the testing circuit and a schematic of the design are included in Section 2. The data for this project was to be collected by a National Instruments 24-bit Analog-to-Digital Converter (ADC) and two 16-bit lock-in amplifiers. Further information about the data acquisition and the initial testing is given in Section 3. The data was then processed after each experiment in MATLAB by Dr. S. Errede and plots of the quantities of interest (complex reactance and complex capacitance) were generated. The results of experiments on four different types of capacitors are given in Section 4.

2 The Circuit

The capacitors needed to be mounted in some sort of circuit for testing, both to acquire data and to simulate operating conditions. The two channels of data acquired from each pair of identical capacitors was the voltage output and current output (with the current being calculated from voltage across a metal-film resistor). The following circuit diagram in Figure 1 was designed by Dr. S.Errede and shows the schematic of the testing circuit.

To avoid introducing noise into the circuit and to provide a high input impedance for the signals from the capacitors, two AD694 low-noise instrumentation op-amps were used to buffer the signal from the circuit to the ADC. These op-amps have high noise-immunity and a large bandwidth to facilitate measurements over the $20Hz - 20kHz$ input frequency testing range.

The data outputs for voltage and current signals is connected to the data collection device via two BNC connectors on the outside of the circuit box. The output signals are extremely sensitive to noise so it was necessary to ensure the circuit itself was adequately shielded against ambient electromagnetic noise, such as the significant $60Hz$ noise produced by power lines. This was done by grounding the metal circuit box to function as a Faraday cage (when the lid is closed during measurements).

Since a direct measurement of current for this circuit would be impractical (such as that obtained by using a clamp meter or some other device that does not directly contact the wires carry the signal), the current measurement was done by measuring the voltage across a 100.0Ω metal-film resistor and using $V = IR$ to obtain the current signal. It was important to use a metal-film resistor rather than a more common carbon-composition resistor to minimize contact noise. Contact noise is usually the largest contribution to noise from resistors and is especially large at low frequencies (owing to the $\frac{1}{f}$ frequency spectrum of contact noise).

The high bias voltage across the two capacitors was supplied by an external power supply hooked up to a MHV connector on the outside of the box. An MHV connector was chosen both to prevent disastrous accidental connection of the high voltage to the BNC data outputs and because MHV connectors are rated for high voltages (3000V and 3A).

The input AC signal used to simulate the input signal across the capacitors comes from an external

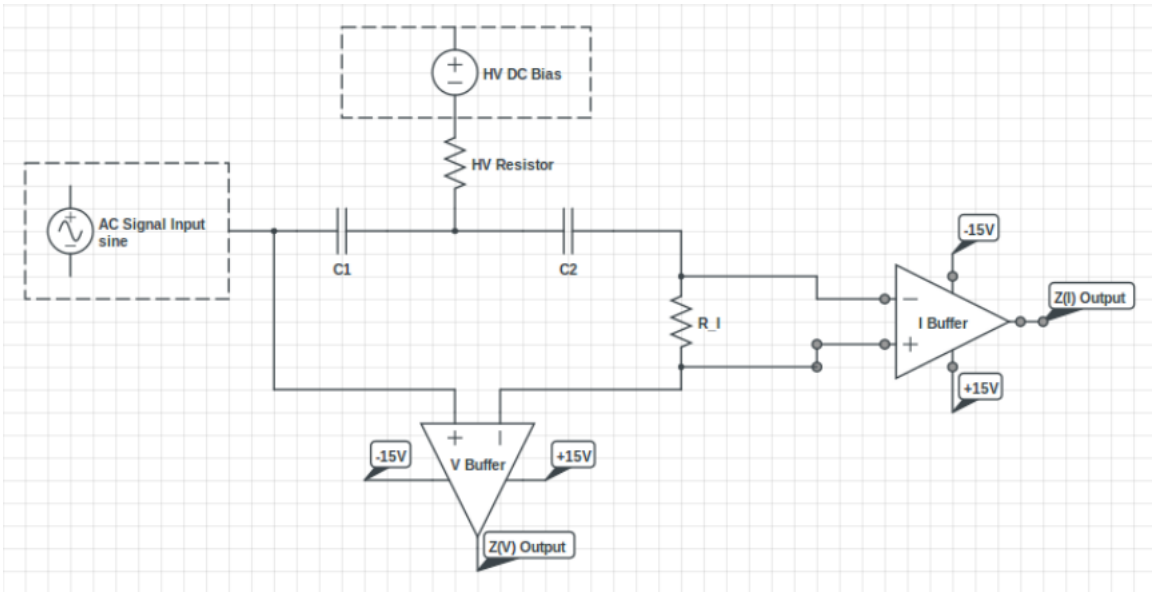

Figure 1: The circuit diagram for the capacitor testing circuit.

signal generator (either a function generator during initial testing or the internal oscillator of the lock-in for measurements). The input signal is hooked up to the circuit via a BNC connector on the outside of the box.

To simulate the conditions that a capacitor would experience when installed in the musical paraphernalia was important during the design of the testing circuit. It was vital to ensure that certain effects that contribute greatly to the response of capacitors under operating conditions were not overly obscured or diminished under testing conditions. For example, the operating condition that was desirable to simulate was the high bias voltage across capacitors that is present when in capacitors installed in various tube amplifiers and guitar amplifiers. To see why this would be an important quantity to simulate, it is necessary to consider what non-ideal capacitor behavior a high bias voltage can induce. The charge on a capacitor is directly proportional to the capacitance and the voltage ($Q = CV$). The amount of charge becomes important when considering leakage current, which is electrically equivalent to a resistor in parallel with the capacitor. In vacuum tube amplifiers, the interstage coupling capacitors that conduct the signal from the high-voltage grid of one tube to the plate of the next tube are particularly prone to leakage currents. These leakage currents can cause excessive current or signal distortion and would influence the sound of the signal significantly. Under low voltages, this leakage current is smaller and thus distortion due to leakage currents would be much smaller and harder to detect than under high bias voltages.

The circuit itself was built on non-conductive, perforated vector board to facilitate soldering of the through-hole components. The non-conductive properties of the vector board made it necessary to cover the board with strips of copper tape before assembly in order to form a ground plane. The large area of the ground plane both made it convenient to ground nodes in the circuit locally and provided some immunity from electrical noise that could be produced via coupling between one part of the circuit and another. The gaps between copper strips were soldered over to ensure a good electrical connection.

A picture of the completed circuit in its case is shown in Figure 2 .

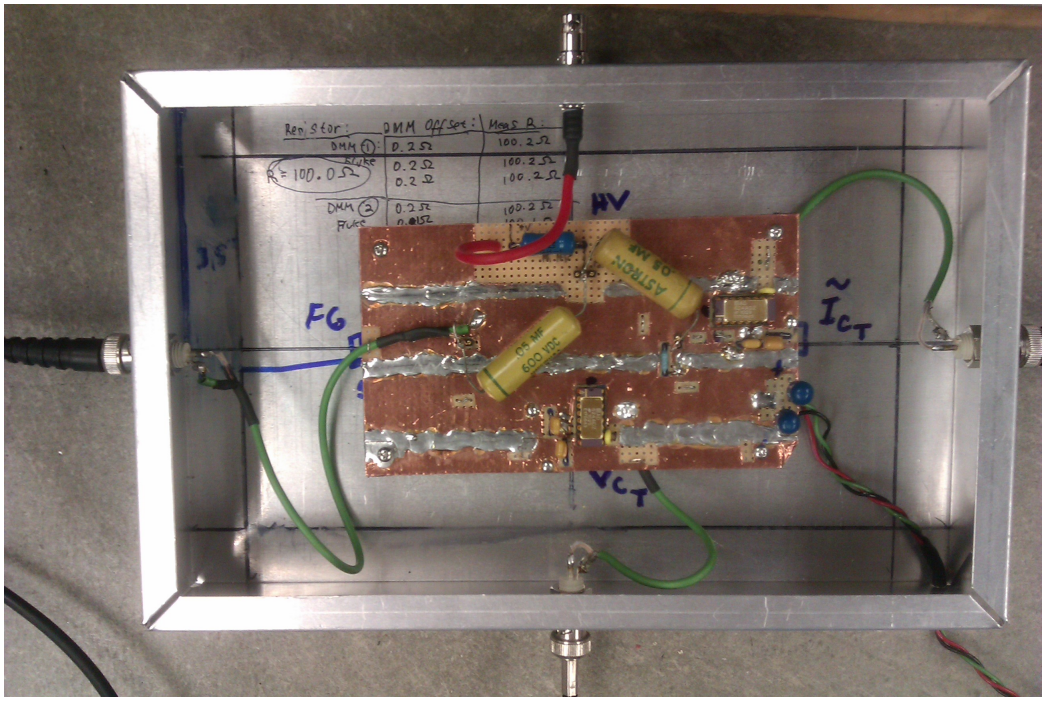

Figure 2: The built capacitor measurement circuit with metal cover off (showing two Astron capacitors soldered in).

3 Initial Testing and Data Acquisition Setup

A test run of the circuit was done after assembly and before a data run was preformed in order to ensure that the circuit was working as intended. For this test, two Astron capacitors were soldered to the capacitor terminals and a $300V$ bias voltage was applied. A picture showing the setup for the test run is given in Figure 3. A picture of the oscilloscope trace and function generator (set to a $f = 17kHz$ sine-wave for testing) during the test run is given in Figure 4.

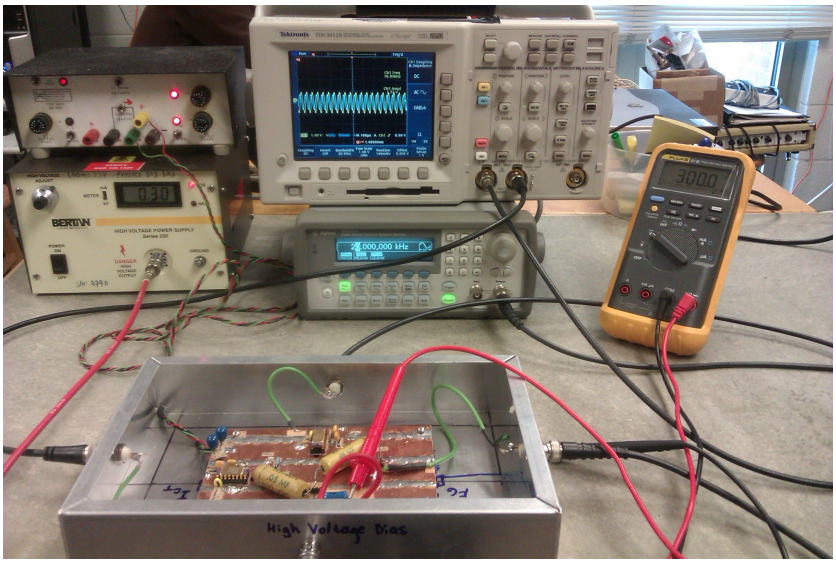

Figure 3: Picture of circuit during the test run. Showing circuit power supply and high-voltage power supply (top left), oscilloscope and signal generator (top middle), and digital multimeter reading the voltage $V = 300\,V$ coming into the high-voltage cable (top right).

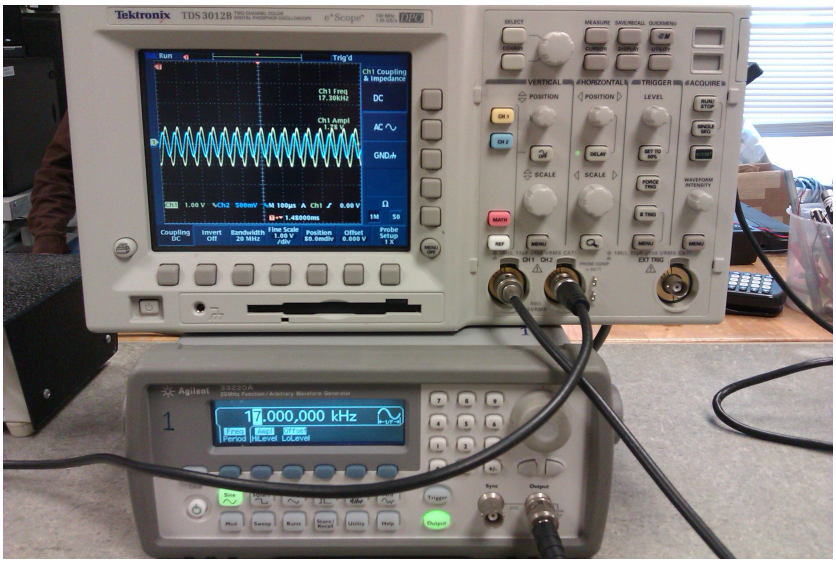

Figure 4: Picture of oscilloscope, showing the yellow voltage trace and blue current trace, (top) and function generator (bottom) during test run.

From Figure 4, it can be seen that under test conditions, the output signal of the circuit indicates that the testing circuit is behaving as expected. The yellow trace on the oscilloscope is the voltage output and

the blue trace is the current output. It can be seen that the current signal lags behind the voltage signal by 90° (a quarter-period) as is expected and that both traces are sinusoids with roughly the same frequency as the input.

After the test run, the circuit was hooked up to the NI ADC and two lock-in amplifiers. A three hour frequency sweep from $20Hz$ to $20kHz$ was preformed to acquire the raw data necessary to extract the quantities of interest.

The actual code used to preform the frequency sweep and control data acquisition is a separate project by Nicholas D'Anna and Dr. S. Errede. Interested parties are referred to the project report 'Data Acquisition with the PXIe-4492' for more detailed information about the data acquisition.

A picture of the LabWindows/CVI panel for the complex capacitance test runs (showing settings and parameters used) is given in Figure 5.

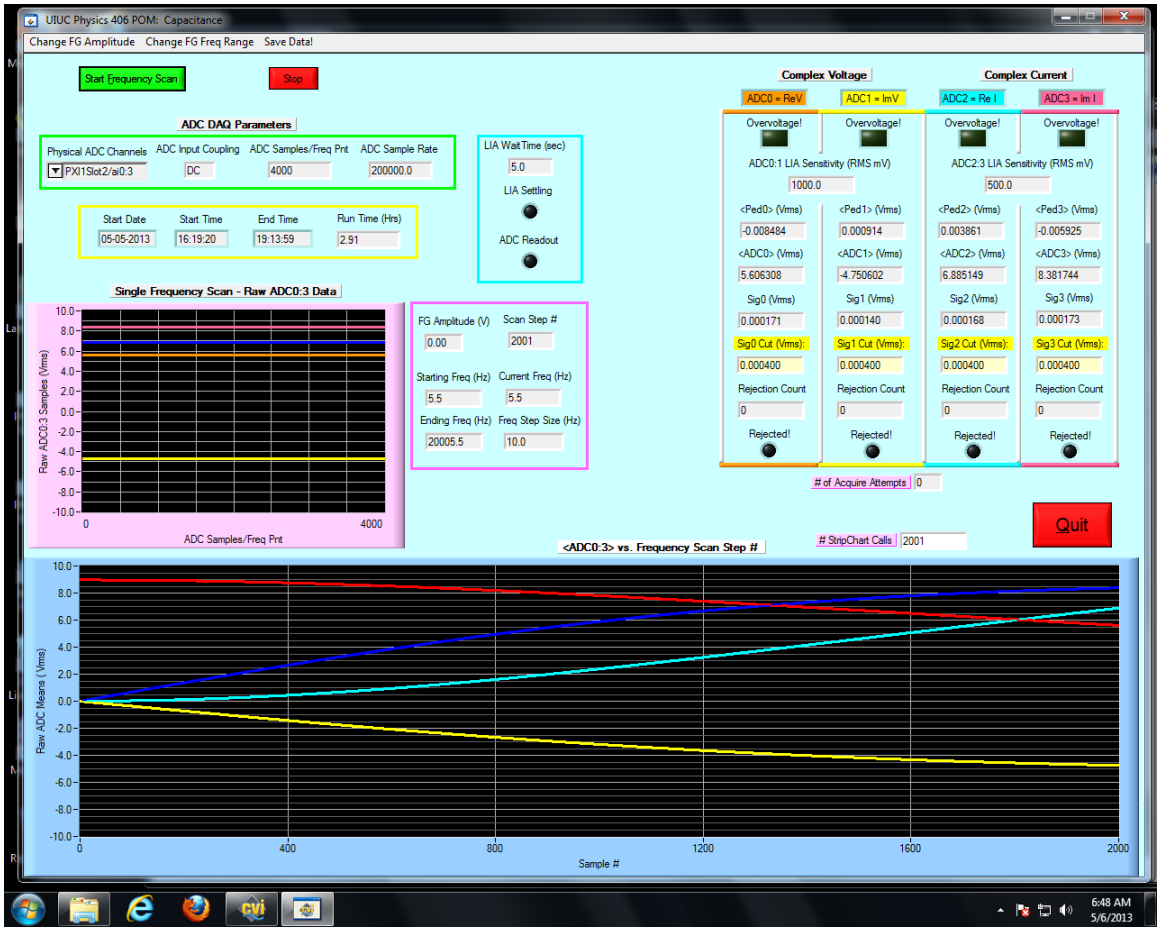

Figure 5: Screen shot of the LabWindows/CVI panel used for capacitance data acquisition.

4 Results

At the time of writing, four pairs of different types of capacitors have been successfully measured. A picture of the capacitors measured and discussed in this report is given in Figure 6.

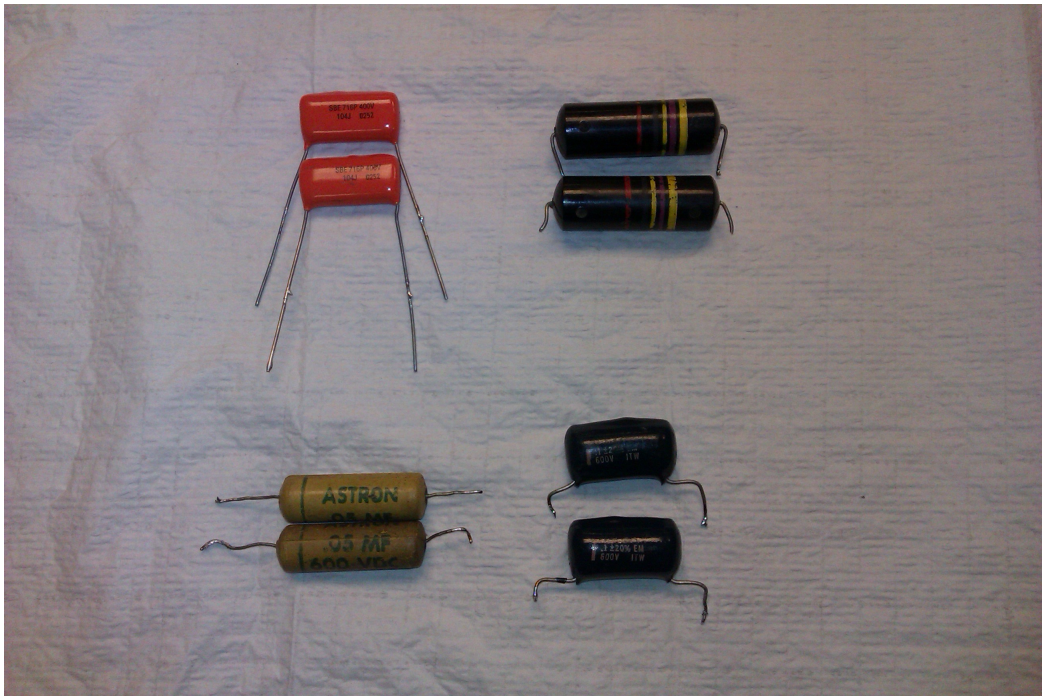

Figure 6: The capacitor pairs that were measured. (Clockwise from top left) Sprague 716P $0.1\mu F$ Orange Drop, Bumblebee $0.47\mu F$, Silver Face Fender $0.1\mu F$ Blue Drop, Astron $0.05\mu F$.

The two quantities acquired from these capacitor tests were both in the frequency-domain: the complex impedance and the complex capacitance.

The complex impedance, $\tilde{Z}_c$, characterizes the response of the opposition of the capacitor to the flow of current when a voltage is applied. It can be seen that the the complex impedance depends on the other quantity measured; the complex capacitance ($\tilde{C}$).

$$\tilde{Z}_c = R_c - i \cdot X_c = \left(\frac{1}{\omega \cdot Im\{\tilde{C}\}}\right) - i\left(\frac{1}{\omega \cdot Re\{\tilde{C}\}}\right)$$

$$\tilde{C} = C_{real} + i \cdot C_{imaginary} = Re\{\tilde{C}\} + i \cdot Im\{\tilde{C}\}$$

The resistance-like part of the impedance is the real part of $\tilde{Z}_c$ and results in the output voltage and output current waveforms being proportional and in phase. For ideal capacitors, this part is equal to zero.

The reactance part of the impedance is the imaginary part of $\tilde{Z}_c$ and results in the output voltage and output current waveforms being out of phase. This part is zero for ideal resistors and non-zero for ideal capacitors and ideal inductors.

For an ideal capacitor, the ideal complex impedance is purely imaginary and dependent on the real part of the complex capacitance.

$$\tilde{Z}_{c,ideal} = R_{c,ideal} - i \cdot X_{c,ideal} = 0 - i \cdot \left(\frac{1}{i\omega C}\right) = -i \cdot \left(\frac{1}{i\omega C_{real}}\right)$$

Also for an ideal capacitor, the ideal complex capacitance is purely real and equal to the usual measured capacitance.

$$\tilde{C}_{ideal} = C_{real,ideal} + i \cdot C_{imaginary} = C + i \cdot 0$$

However, for non-ideal capacitors, $Im\{\tilde{C}\}$ is not zero and arises (at least in dielectric capacitors) from momentary lag in the dielectric constant of the material. This lag is caused by the time delay in the response of polarized molecules to a changing electric field and is dependent on frequency. In a real capacitor, this is expected if it is remembered that a material cannot respond instantaneously to a change in the applied field. To maintain a causal relationship, any response of the dielectric must happen after the field is applied and this can be represented as a phase difference. The phase difference is suggestive of a complex quantity and leads to the necessity of an imaginary part of the capacitance.

Graphs of each quantity measured (complex capacitance and complex impedance) for each type of capacitor are shown and discussed in the following subsections.

4.1 Sprague 716P $0.1\mu F$ Orange Drop

The Sprague 716P 'Orange Drop' capacitors measured are modern capacitors used primarily in guitar amplifiers. They are noted for sounding 'transparent', meaning they do not significantly change the musical qualities of a signal.

4.1.1 Orange Drop Complex Impedance

In Figure 7, the results of the complex impedance testing of two Orange Drop capacitors are shown.

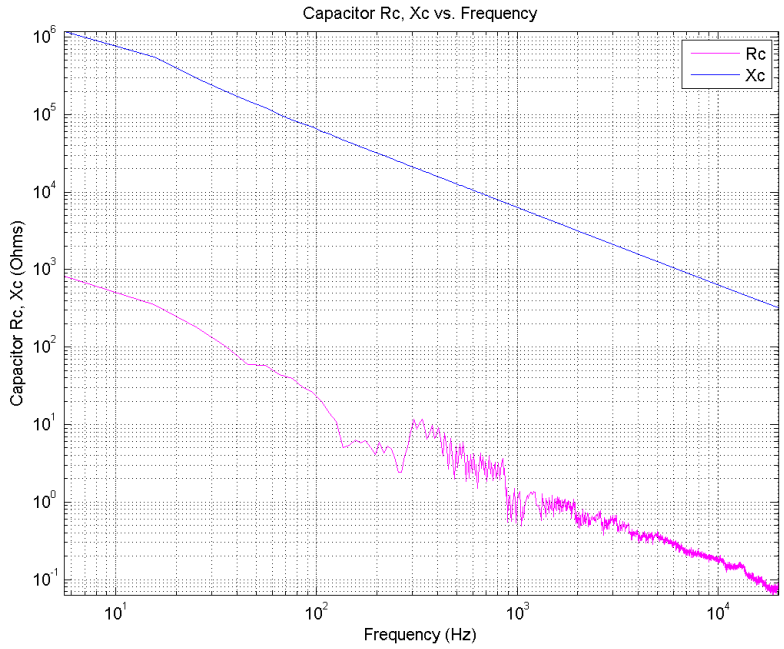

Figure 7: Graph of Orange Drop impedance $\tilde{Z}_c$ ($\tilde{Z}_c = R_c + iX_c$) versus frequency. The top, blue line shows X_c, the imaginary part of impedance and the bottom, magenta line shows R_c, the real part of impedance.

It can be seen that the ratio of the real and imaginary parts of the impedance at low frequencies was 10^3 and the ratio at high frequencies was closer to 10^4. The imaginary part was smooth and linearly decreasing with frequency. The real part, in contrast, was not smooth and had some spikes in impedance. It can be seen that the real and imaginary impedance lines are not parallel since they diverge by a factor of 10 in capacitance over four decades in frequency.

4.1.2 Orange Drop Complex Capacitance

In Figure 8, the results of the complex capacitance testing of two Orange Drop capacitors are shown.

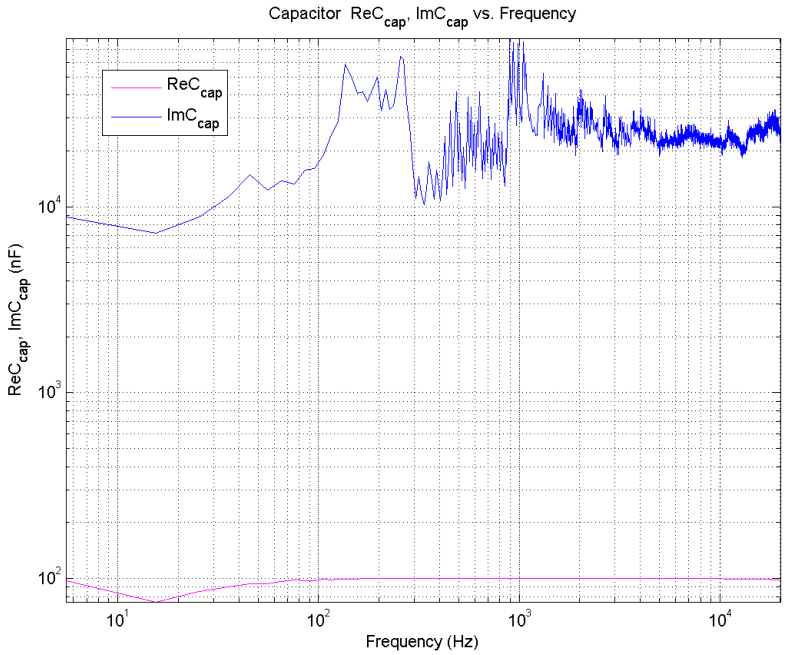

Figure 8: Graph of complex capacitance $\tilde{C}_{cap}$ (where $\tilde{C}_{cap} = Re\{\tilde{C}_{cap}\} + i \cdot Im\{\tilde{C}_{cap}\}$) versus frequency for the Orange Drop. The top, blue line plots the imaginary part, and the bottom, magenta line plots the real part.

The complex capacitance of the Orange Drop capacitors is similar to the complex capacitance of the Blue Drop capacitors (Section 4.3.2) and Astron capacitors (Section 4.4.2).

The real part of the capacitance begins at a value of $100nF$, dips slightly to $70nF$ at about $15Hz$, and then rises again to $100nF$ at $100Hz$. At higher frequencies, the real part of the capacitance maintains a value of $100nF$ over the rest of the frequency range. The imaginary part has many large ($\sim 5 \cdot 10^4\, nF$) spikes and fluctuates between a maximum of $1.7 \cdot 10^4\, nF$ and a minimum of $7 \cdot 10^3\, nF$. The fluctuations are much more rapid at higher frequencies.

4.2 Bumblebee $0.47\mu F$

The Bumblebee capacitors measured are vintage capacitors made in the 1950's that were used primarily in tone control circuits of Gibson guitars. They are noted for their very pleasing musical properties and are highly desired by guitar aficionados for the superior sound they produce.

4.2.1 Bumblebee Complex Impedance

In Figure 9, the results of the complex impedance testing of two Bumblebee capacitors are shown.

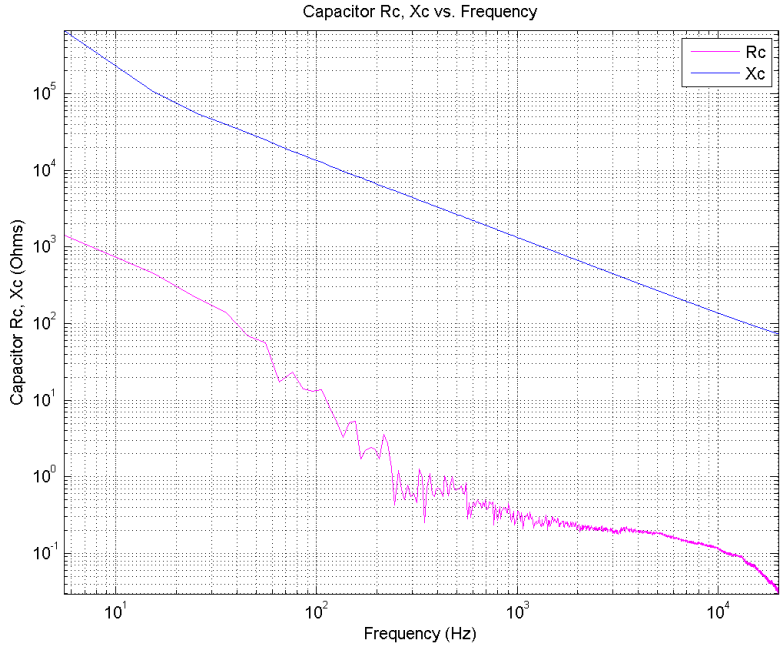

Figure 9: Graph of Bumblebee impedance $\tilde{Z}_c$ ($\tilde{Z}_c = R_c + iX_c$) versus frequency. The top, blue line shows X_c, the imaginary part of impedance and the bottom, magenta line shows R_c, the real part of impedance.

The imaginary part looks very smooth and begins at a value of $6 \cdot 10^5\Omega$. It decreases smoothly with increasing frequency to a value of $8 \cdot 10^1\Omega$ at high frequencies. The real part begins at a value of about $10^3\Omega$ and looks to be smoothly decreasing with frequency at the low end of the frequency range tested but begins to display rapid oscillations at $30Hz$, after which the real part decreases more sharply than linearly with frequency. The real part of the complex impedance ends at a value of about $3 \cdot 10^{-2}\Omega$.

The imaginary part and real part of the impedance differ by a factor of 10^2 at low frequencies and 10^3 at high frequencies, indicating that the real and imaginary parts are not parallel and do not have the same frequency dependence.

4.2.2 Bumblebee Complex Capacitance

In Figure 10, the results of the complex capacitance testing of two Bumblebee capacitors are shown.

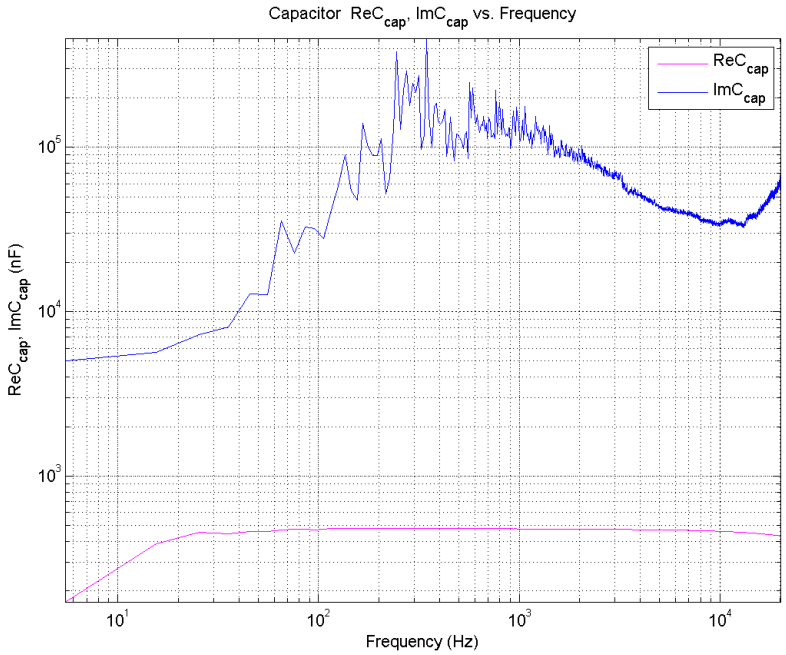

Figure 10: Graph of complex capacitance $\widetilde{C}_{cap}$ (where $\tilde{C}_{cap} = Re\{\tilde{C}_{cap}\} + i \cdot Im\{\tilde{C}_{cap}\}$) versus frequency for the Bumblebee. The top, blue line plots the imaginary part, and the bottom, magenta line plots the real part.

The real part of the complex capacitance begins at a value of about $200nF$ and rises smoothly to the steady value of $500nF$ that is maintained over the rest of the frequency range. The imaginary part of the complex capacitance begins at a value of $1300nF$ at low frequencies and rises smoothly until $30Hz$, after which it begins to display the rapid oscillations that were seen in the imaginary capacitance of the other types of capacitors tested.

4.3 Silverface Fender $0.1\mu F$ Blue Drop

The Silverface-era Fender 'Blue Drop' capacitors are another type of vintage capacitor. They were made in the 1970's by the company CBS and used in Fender guitar amplifiers. They are classified as 'muddy' sounding and are not considered to have good musical properties.

4.3.1 Blue Drop Complex Impedance

In Figure 11, the results of the complex impedance testing of two Blue Drop capacitors are shown.

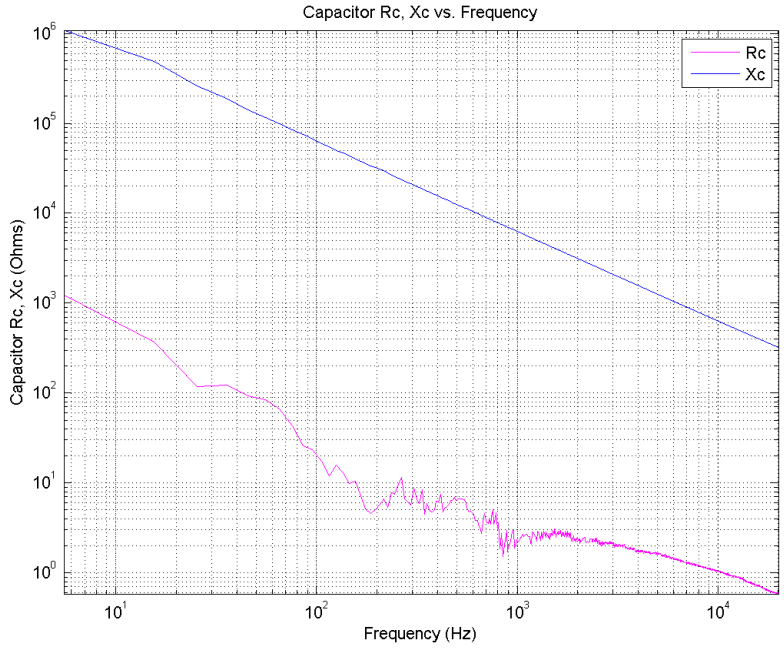

Figure 11: Graph of Blue Drop impedance $\tilde{Z}_c$ ($\tilde{Z}_c = R_c + iX_c$) versus frequency. The top, blue line shows X_c, the imaginary part of impedance and the bottom, magenta line shows R_c, the real part of impedance.

The real part of the complex impedance has an initial value of $10^6\Omega$ at low frequencies and decreases smoothly with increasing frequency to a value of about 200Ω at high frequencies. The imaginary part of the complex impedance begins at a value of $10^3\Omega$ and decreases to about 1Ω at high frequencies. The ratio between the real and imaginary parts of the complex impedance is about 10^3 at low frequencies and 10^2 at high frequencies, indicating that the real and imaginary parts are not parallel and do not have the same frequency dependence.

4.3.2 Blue Drop Complex Capacitance

In Figure 12, the results of the complex capacitance testing of two Blue Drop capacitors are shown.

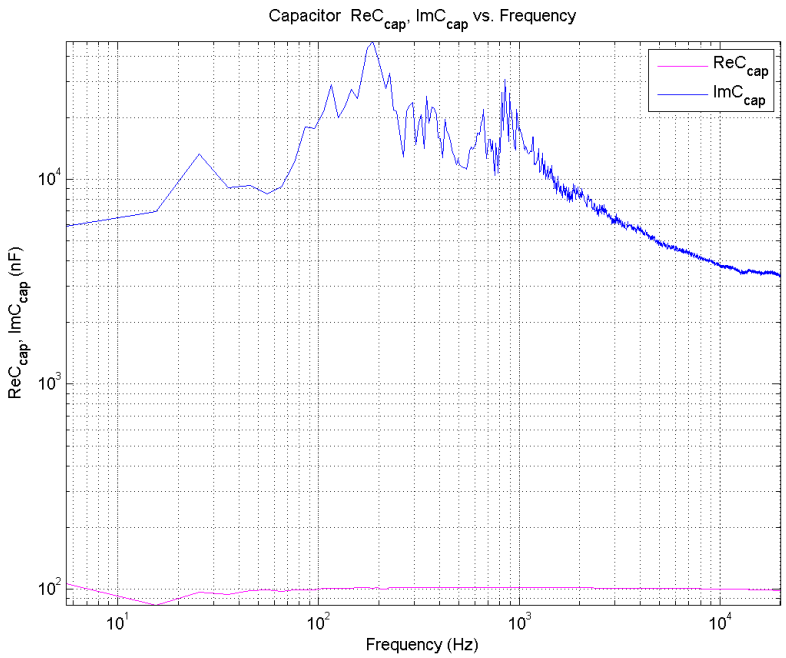

Figure 12: Graph of complex capacitance $\widetilde{C}_{cap}$ (where $\tilde{C}_{cap} = Re\{\tilde{C}_{cap}\} + i \cdot Im\{\tilde{C}_{cap}\}$) versus frequency for the Blue Drop. The top, blue line plots the imaginary part, and the bottom, magenta line plots the real part.

The complex capacitance of the Blue Drop capacitors is similar to the complex capacitance of the Orange Drop capacitors (Section 4.1.2) and Astron capacitors (Section 4.4.2).

The real part of the capacitance begins at a value of $100nF$, dips slightly to $80nF$ at about $15Hz$, and then rises again to $100nF$ at $25Hz$. At higher frequencies, the real part of the capacitance maintains a value of $100nF$ over the rest of the frequency range. The imaginary part has many large ($\sim 10^4\, nF$) spikes and fluctuates between a maximum of $1.4 \cdot 10^4\, nF$ and a minimum of $3 \cdot 10^3\, nF$. The fluctuations are also much more rapid at higher frequencies.

4.4 Astron $0.05\mu F$

The Astron capacitors are another type of vintage capacitor. Astron capacitors were made in the 1950's and were used in tweed Fender guitar amplifiers. They are noted for having a very good musical sound and are pleasing to listen to.

4.4.1 Astron Complex Impedance

In Figure 13, the results of the complex impedance testing of two Astron capacitors are shown.

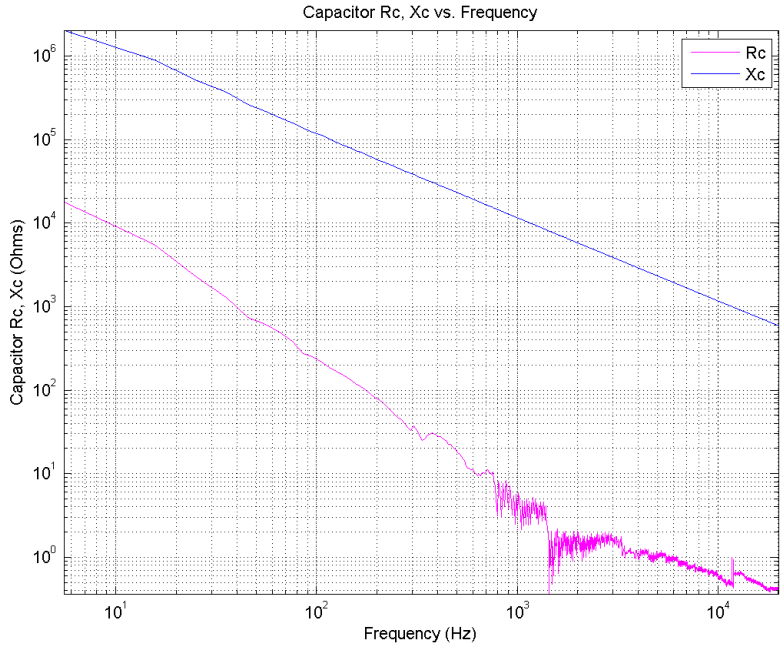

Figure 13: Graph of Astron impedance $\tilde{Z}_c$ ($\tilde{Z}_c = R_c + iX_c$) versus frequency. The top, blue line shows X_c, the imaginary part of impedance and the bottom, magenta line shows R_c, the real part of impedance.

The real part of the complex impedance begins with a value of $2 \cdot 10^4 \Omega$ at low frequencies and decreases without very many capacitance spikes until $6 \cdot 10^2 Hz$, after which the real impedance shows rapid oscillations until ending at a value of $4 \cdot 10^{-1} \Omega$. The imaginary part of the complex impedance begins with a value of $2 \cdot 10^6 \Omega$ and decreases smoothly with frequency over the frequency range measured to a final value of $6 \cdot 10^2 \Omega$. The ratio between the real and imaginary parts of the complex impedance at low frequencies is about 10^2 and the ratio at high frequencies is about 10^3 indicating that the real and imaginary lines are not parallel.

4.4.2 Astron Complex Capacitance

In Figure 14, the results of the complex capacitance testing of two Astron capacitors are shown.

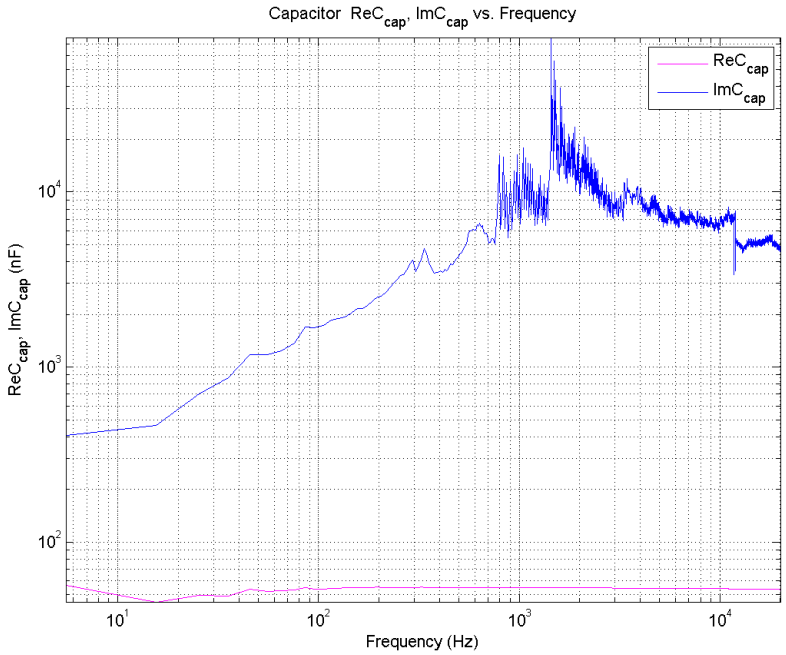

Figure 14: Graph of complex capacitance $\widetilde{C}_{cap}$ (where $\tilde{C}_{cap} = Re\{\tilde{C}_{cap}\} + i \cdot Im\{\tilde{C}_{cap}\}$) versus frequency for the Astron. The top, blue line plots the imaginary part, and the bottom, magenta line plots the real part.

The complex capacitance of the Astron capacitors is similar to the complex capacitance of the Orange Drop capacitors (Section 4.1.2) and Blue Drop capacitors (Section 4.3.2).

The real part of the complex capacitance begins at a value of $6 \cdot 10^1 nF$ and dips to a value of $4.5 \cdot 10^1 nF$ at $15Hz$. It rises again to $6 \cdot 10^1 nF$ at $45Hz$ and maintains that value over the rest of the frequency range. The imaginary part of the complex capacitance begins at a value of $4 \cdot 10^2 nF$ and rises with some discontinuities until $5 \cdot 10^3 nF$ at $300Hz$, after which it displays the same large spikes present in the other complex capacitance measurements until settling at a final value of $5 \cdot 10^3 nF$ at high frequencies.

5 Conclusion and Future Work

The current measurements and acquired data for the complex impedance and complex capacitance of four different capacitors are interesting and of good quality. However, the current body of data does not reveal striking differences between 'musical' capacitors and 'dud' capacitors. The author does not have enough knowledge on the subject to put forth her own hypotheses about the results presented for each capacitor type and their correlation with the musical properties of that type of capacitor but that is a possible avenue for future work. The other, more promising, avenue for future work is to take time-domain measurements on the capacitors using a spectrum analyzer. This could reveal the distortions to an input signal across the capacitor very plainly. Making time-domain measurements would also pick up any harmonics that are introduced in the distortions. Since the harmonic content of a musical sound heavily influences how it is perceived (particularly timbre/sound quality) analyzing the harmonic content of distortions could yield more decisive correlations between measurements and musical properties.

In conclusion, more data is needed on different types of capacitors before any conclusion can be made on the frequency-domain measurements of musical properties of capacitors. Additionally, time-domain measurements should be preformed before a firm statement about the correlation between time-domain measurements and the 'musicality' of capacitors is made.